Four-Channel Spatial Multiplexing Over a Millimeter-Wave Line-of-Sight Link

Colin Sheldon, Munkyo Seo, Eric Torkildson, Mark Rodwell, and Upamanyu Madhow

Department of Electrical and Computer Engineering, University of California, Santa Barbara, CA 93106

***Abstract* — A scalable system architecture is proposed and demonstrated for spatial multiplexing over millimeter-wave line-of-sight communication links. This architecture provides increased data capacity without increasing the channel bandwidth. The modulation format is simple (BPSK or QPSK); this facilitates high-rate operation. The spatially multiplexed channels are separated at the receiver using broadband adaptive analog I/Q vector signal processing, a technique which should readily scale to data rates exceeding 10 Gb/s per channel. A control loop continuously tunes the channel separation electronics to correct for changes with time in either the propagation environment or the system components. Design and characterization of a four channel 60 GHz hardware prototype is presented.**

***Index Terms* — Channel separation, Line-of-Sight wireless link, millimeter-wave radio communication, MIMO systems, spatial multiplexing.**

I. Introduction

Radio links employing spatial multiplexing provide increased communication link data capacity without increased channel bandwidth. Research in this area has focused primarily on non line-of-sight links operating at low GHz carrier frequencies [1] and aggregate data rates below 1 Gb/s.

An alternative approach applies spatial multiplexing to a line-of-sight (LOS) link [2]. For spatially multiplexed links using linear arrays of a fixed total length, the maximum number of spatially multiplexed channels varies as the inverse of carrier wavelength λ; for rectangular arrays the maximum number of channels varies as $1/\lambda^2$. In the 57-64 GHz, 71-76 GHz, and 81-86 GHz mm-wave bands, the short wavelengths permit a large number of spatial channels while the large available bandwidths permit a high data rate per spatial channel; aggregate data transmission rates far exceeding 10 Gb/s are thus feasible.

LOS spatial multiplexing [3] exploits the principles of diffraction-limited optics. The transmitter and receiver use either $1\times n$ linear or $n\times n$ rectangular antenna arrays whose elements are separated by a distance D, selected to ensure the angular separation of the transmitter elements is greater than or equal to the angular resolution of the receiver array. This condition leads to the relationship

$$D = \sqrt{R \cdot \lambda / n}\,, \qquad (1)$$

where D is the antenna element spacing and R is the link range [2].

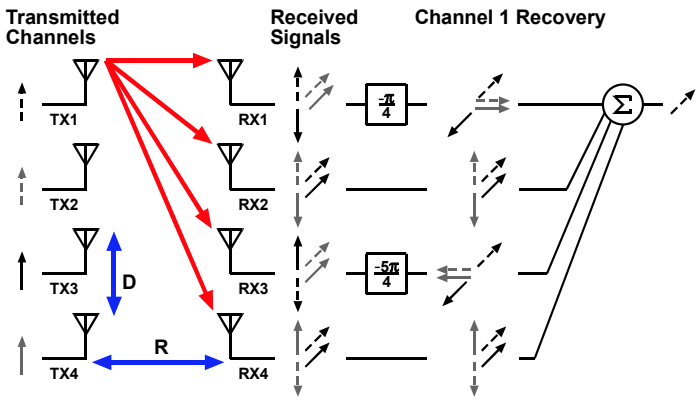

Fig. 1. Signal propagation and a channel recovery example for an ideal four channel line-of-sight spatially multiplexed link. Transmitted and received signals are represented as vectors in the I/Q plane.

LOS spatially multiplexed links can be analysed by calculating the relative phase shifts experienced by the signal vectors as they propagate between the antenna arrays (Fig. 1). The system is characterized by a channel matrix H whose (normalized) elements $h_{m,n}$ correspond to the complex channel gain from the m^{th} transmitter element to the n^{th} receiver element. If channel losses are equal, then

$$h_{m,n} = e^{-i\frac{2\pi}{\lambda}(d(m,n)-R)}\,, \qquad (2)$$

where $d(m,n)$ is the distance between the m^{th} transmitter and the n^{th} receiver elements [2]. Inverting this channel matrix and applying it to the array of received signals separates the individual channels. LOS links with linear and rectangular arrays are robust to small deviations in individual antenna alignment and array positioning [2], [4], [5].

We have previously reported experimental results from a 60GHz hardware prototype using 1×2 linear arrays and a manually-tuned channel separation network operating in the receiver's IF section [6], [7]. These results demonstrated the feasibility and performance potential for LOS spatial multiplexing at millimeter-wave frequencies.

This paper reports experimental results from a 60 GHz hardware prototype demonstrating LOS spatial multiplexing using 1×4 linear arrays. Channels are now separated by converting the received signals to baseband and forming linear combinations of their I and Q components, an approach which more readily scales to a large number of channels. The

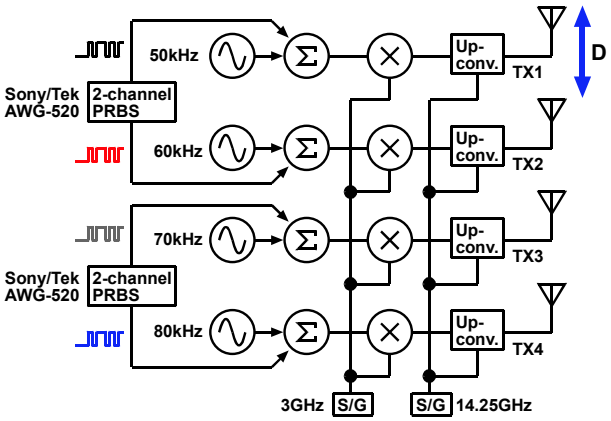

Fig. 2. Transmitter prototype block diagram.

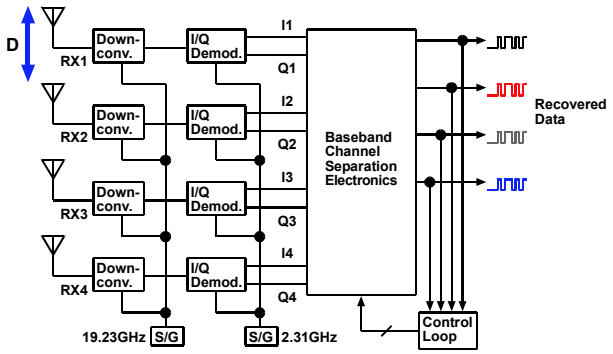

Fig. 3. Receiver prototype block diagram.

channel separation hardware is continuously and adaptively tuned under closed-loop digital control. Section II reviews the design of the hardware prototype and control loop. The following section presents results from indoor experiments over a 5 m link range.

II. Baseband Channel Separation Prototype

The hardware prototype (Figs. 2-5) uses commercially available mm-wave and RF components and a printed circuit board based channel separation network. The prototype consists of a four element (1×4) transmitter and a four element receiver.

A. Transmitter

The transmitter prototype (Fig. 2) consists of baseband data sources, pilot tone sources, BPSK modulators, and 60 GHz upconverters. The baseband data sources generate four independent Pseudo Random Bit Sequences (PRBS) with sequence length 2^{17}-1. Each PRBS sequence has a different maximal length shift register feedback configuration so that we can conclusively show the receiver separates channels correctly. Unique pilot tones are added to each PRBS sequence and the combined signal is applied, in bipolar format, to the baseband port of a mixer operating with a 3 GHz local oscillator. A second mixer upconverts the 3 GHz BPSK signal to 60 GHz. The mixer image response and LO feedthrough are both suppressed by a 58-62 GHz bandpass filter. Each transmitter uses a 24 dB_i standard gain horn antenna.

B. Receiver Electronics

The receiver prototype (Fig. 3) contains 60 GHz downconverters, I/Q demodulators, baseband channel separation electronics, and a control loop. The 60 GHz downconverter modules bring the received signals down to a 2.31 GHz IF frequency. They each consist of a 24 dB_i standard gain horn antenna, bandpass filter, and a mixer. I/Q demodulators bring the received signals down to baseband.

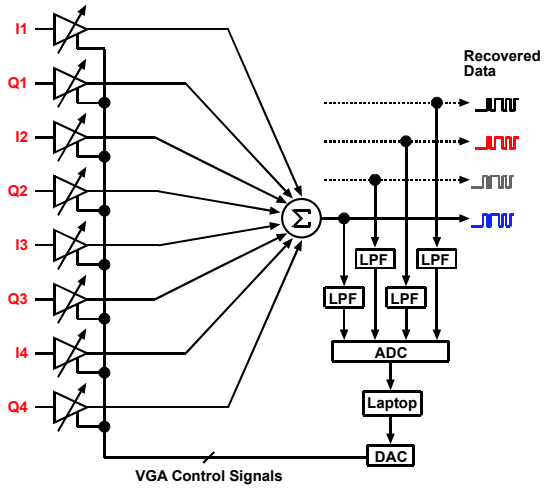

Fig.4. Baseband channel separation circuit board and control loop schematic.

Signal splitters distribute the baseband I and Q signals to a pair of channel separation circuit boards (Fig. 4). The channel separation PCBs consist of arrays of variable gain amplifiers (VGAs) and a summation network. Each VGA is a full four-quadrant analog multiplier, allowing arbitrary magnitude scaling and phase shift operations on each of the received signals.

For an ideal system, only phase shift operations are required (Fig. 1) to separate channels at the receiver. A real system will have gain mismatches between individual transmitters and receivers and will also require magnitude scaling. The channel separation network must also be capable of arbitrary phase shift operations to account for antenna positioning errors.

The recovered data was captured on a two channel oscilloscope controlled by a computer. Two recovered channels were simultaneously stored for off line bit error rate (BER) analysis. This initial hardware prototype was only capable of recovering two channels simultaneously but can be expanded to recover all four channels by increasing the number of channel separation circuit boards.

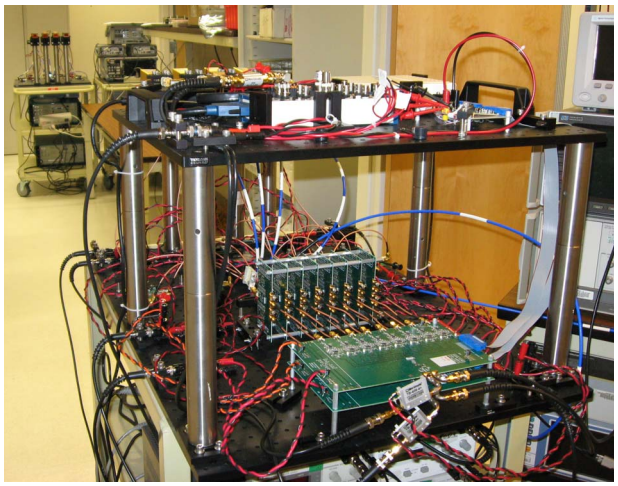

Fig.5. Photograph of the receiver prototype. The vertical PCBs are signal distribution circuits and the horizontal PCBs are the baseband channel separation circuits. The transmitter prototype is visible in the upper left.

Carrier recovery was not implemented at the receiver. A 10 MHz reference signal was shared by the transmitter and receiver local oscillators. This allowed a pair of channel separation circuit boards to simultaneously recover two data channels in real time. Without the shared reference signal, frequency errors at the receiver local oscillators would require final data recovery by Differential PSK (DPSK) demodulation, and would require a more rapid channel adaptation algorithm to compensate for frequency drift of the pilot tones. The effectiveness of DPSK demodulation in a spatially multiplexed mm-wave link has been verified experimentally [6], [7].

C. Receiver Control Loop

The control loop adjusts the baseband VGA coefficients so that the output of the channel separation network (CSN) contains the data stream from the desired transmit channel, while canceling other interfering channels.

First, the output of the CSN is filtered and digitized at 500 Ksamples/s to measure the magnitude of the embedded transmitter pilot tones. Note the sampling rate is determined not by the data rate, but by the pilot frequency, which is below 100 kHz. By performing an FFT operation, the magnitude of each pilot tone can be identified. Specifically, the amount of interference channel power at the receiver k can be quantified by

$$NPP_k = \frac{P_{k,k}}{P_{k,1} + P_{k,2} + P_{k,3} + P_{k,4}}, \qquad (3)$$

where NPP_k is the normalized pilot power at receiver k, and $P_{k,j}$ the pilot power from transmitter j coupled to the receiver k. Upon perfect channel separation, NPP_k will be equal to one,

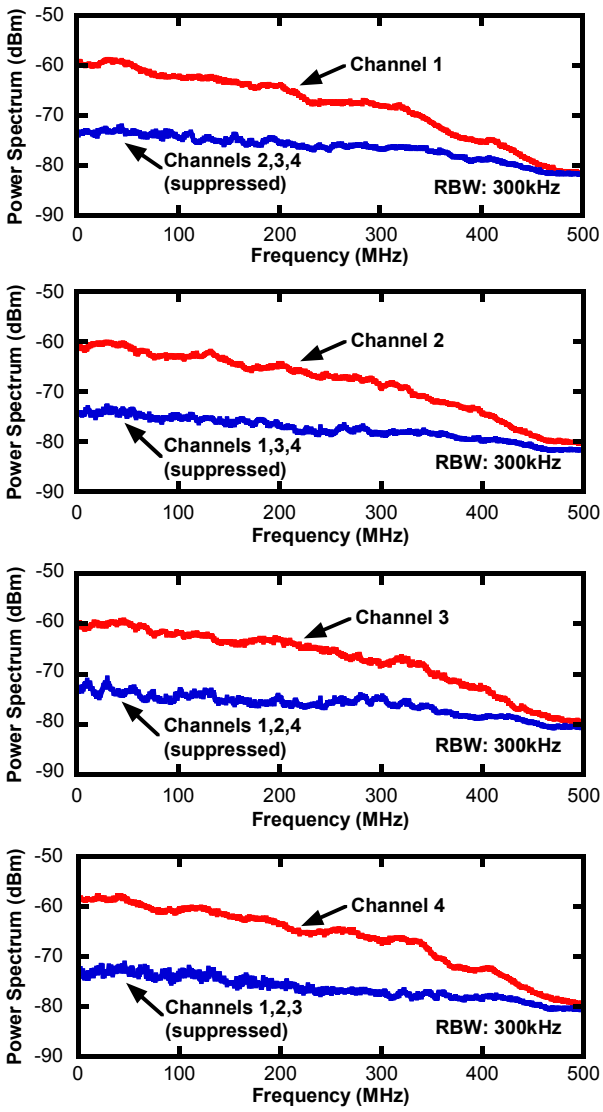

Fig. 6. Measured channel suppression network performance.

with $P_{k,j}=0$ for all $k \neq j$. The control loop attempts to find the optimum tuning of the k-th receiver CSN, $\mathbf{c}_{\mathbf{k},\mathrm{opt}}$, by maximizing the normalized pilot power,

$$\mathbf{c}_{\mathbf{k},\mathrm{opt}} = \arg\max_{\mathbf{c_k}} NPP_k, \qquad (4)$$

where $\mathbf{c}_\mathbf{k} = [c_{1,I}\ c_{1,Q}\ \ c_{2,I}\ c_{2,Q}\ \ldots\ c_{4,I}\ c_{4,Q}]$ represents control voltages for the VGA array at receiver k. The optimization is currently implemented as a gradient-based iteration, where each VGA voltage is iteratively adjusted to the direction of increasing NPP_k. In the current prototype, a single update of all VGA voltages takes on the order of 1 second, allowing for the tracking of slow-varying channel conditions and group delay variations in the receiver electronics.

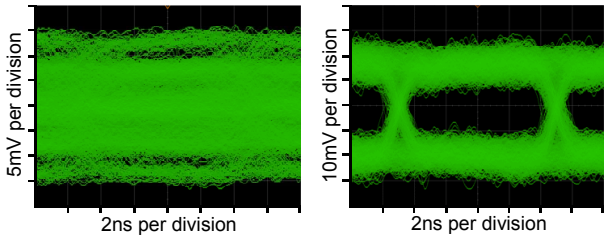

Fig. 7. Receiver eye patterns before (left) and after (right) channel separation.

III. Experimental Results

The hardware prototype was tested in an indoor office environment at a 5 m link range. The antenna element spacing was 7.9 cm at both the transmitter and receiver (Eq. 1). The performance of the baseband channel separation circuits was characterized in the frequency domain and with bit error rate testing.

A. Channel Suppression Measurements

Channel separation network performance was characterized in the frequency domain by transmitting 600 Mbps PRBS sequences. After programming the control loop to recover a particular channel, the received power spectrum was measured at the output of the channel separation network under two conditions.

First, the desired channel was activated. The second measurement was made with the desired channel turned off and the three interference channels activated. Fig. 6 shows the received power spectrum for each channel for both cases. The measured signal-to-interference ratio for each channel is summarized in Table 1. Similar performance was achieved for all recovered channels.

B. Bit Error Rate Testing

The BER performance of the system was measured for two cases. First, a single channel was activated and the BER was measured to obtain the system performance in the absence of interference channels. The second set of BER measurements was performed with all channels active simultaneously to assess the impact of channel separation network performance on transmission error rates.

The tested data rate was 100 Mbps, due to lower than expected receiver bandwidth. For the case of a single active channel, the measured BER was $< 10^{-5}$ for all channels. BER measurement results for the case of all channels active simultaneously are summarized in Table 1. Similar performance was achieved for each recovered channel in both the presence and absence of interference signals. Fig. 7 shows typical receiver eye patterns before and after channel separation.

TABLE I
SUMMARY OF EXPERIMENTAL RESULTS

Recovered Channel	BER	Signal-to-Interference Ratio (dB)
1	$< 10^{-5}$	11
2	1.7×10^{-5}	12
3	$< 10^{-5}$	11
4	$< 10^{-5}$	13

IV. Conclusion

We have demonstrated a scalable architecture for line-of-sight wireless links employing spatial multiplexing. Channel separation at baseband has been demonstrated with a four element prototype. Similar channel separation performance was obtained for all recovered channels. A real time control loop was used to dynamically tune the analog channel separation circuits.

Further work on enhancing the performance of the channel separation electronics, refining the control loop algorithm and implementing differential data demodulation is underway.

Acknowledgement

This work was funded by NSF under grants ECS-0636621 and CNS-0520335. The authors would like to thank C. Patrick Yue for guidance on transistor level circuit design.

References

[1] P. Wolniansky, G. Foschini, G. Golden, and R. Valenzuela, "V-BLAST: an architecture for realizing very high data rates over the rich-scattering wireless channel," *Proc. ISSSE'98*, pp. 295-300, 1998.

[2] E. Torkildson, B. Ananthasubramaniam, U. Madhow, and M. Rodwell, "Millimeter-wave MIMO: Wireless Links at Optical Speeds," *Proc. of 44th Allerton Conference on Communication, Control and Computing*, 2006.

[3] D. Gesbert, H. Bolcskei, D. Gore, and A. Paulraj, "Outdoor mimo wireless channels: models and performance prediction," *IEEE Transactions on Communications*, vol. 50, no. 12, pp. 1926–1934, Dec 2002.

[4] F. Bohagen, P. Orten, and G. Oien, "Construction and capacity analysis of high-rank line-of-sight mimo channels," *IEEE Wireless Communications and Networking Conference,* vol. 1, pp. 432–437, Mar. 2005.

[5] P. Larsson, "Lattice array receiver and sender for spatially orthonormal mimo communication," *61st IEEE Vehicular Technology Conference*, vol. 1, pp. 192–196, May 2005.

[6] C. Sheldon, E. Torkildson, M. Seo, C.P. Yue, U. Madhow, and M. Rodwell, "A 60GHz Line-of-Sight 2x2 MIMO Link Operating at 1.2Gbps," *IEEE International AP-S Symposium*, July 2008.

[7] C. Sheldon, E. Torkildson, M. Seo, C.P. Yue, M. Rodwell, and U. Madhow, "Spatial Multiplexing Over a Line-of-Sight Millimeter-Wave MIMO Link: A Two-Channel Hardware Demonstration at 1.2Gbps Over 41m Range," 2008 European Microwave Convention, October 2008.